EA303 WIND TUNNEL
EXPERIMENT II

TWO DIMENSIONAL
WING PRESSURE DISTRIBUTION AND WAKE SURVEY

I. Purpose

1. To observe the characteristics of the pressure distribution on a two dimensional wing section at various angles of attack including angles of attack above the stall angle of attack.
2. To obtain experimental sectional lift and drag coefficients versus angles of attack, C_l vs α and C_d vs α, and to compare them with those provided by NACA for similar two dimensional wing sections.
3. To observe the characteristics of the wake behind a two-dimensional airfoil, e.g., the local dynamic pressure, the width of the wake, its location, how the wake changes with angle of attack, etc. To observe the effects of angle of attack on the surface pressure distribution around the airfoil.
4. To apply the linear momentum theorem to an arbitrary volume enclosing the airflow over the airfoil and its wake, and to determine the sectional drag coefficient of the airfoil in a real fluid without any direct measurements on the model, i.e., without a balance or surface pressure measurement.

II. References

1. White, F. M., *Fluid Mechanics*, McGraw-Hill, 2nd edition, 1986, pp. 132–142.
2. Kuethe and Chow, *Foundations of Aerodynamics*, Wiley 1986, pp. 64–70.
3. Abbott, Ira H. and Von Doenhoff, Albert, E, *Theory of Wing Sections*, Dover 1959, pp. 1–30, 124–187.
4. Rae and Pope, *Low-Speed Wind Tunnel Testing*, Wiley 1984, pp. 213–222.

III. Introduction

A two-dimensional wing is one whose shape, flow pattern, and sectional properties do not vary in a direction normal to the plane of the flow. Theoretically, this two dimensional flow exists only on a wing of infinite aspect ratio ($AR = \infty$), i.e., when the ratio of the wing span divided by the mean aerodynamic chord is infinite. In practice, it is approached on the interior portion of an extremely long wing or a wing mounted wall-to-wall in a wind tunnel test section. The exterior portions of the wing are excluded to avoid tip effects — caused by the trailing tip vortices which result from the three dimensional flow over a finite wing — and wall boundary layer effects. Knowledge of two-dimensional airfoil properties is extremely important because they are an integral part of the analysis of the three dimensional flow characteristics over a finite wing.

The two dimensional drag which occurs in a real fluid is called profile drag. It is composed of pressure (or form) drag and skin friction (or viscous) drag. Form drag is due mainly to pressure differences between the forward and aft portions of the airfoil (body) caused by boundary layer separation. Skin friction (or viscous) drag is caused by shear stresses on the surface of the body.

The form (pressure) drag coefficient can be determined by integrating the streamwise components of the surface pressure coefficients calculated using data obtained from static pressure taps located around the circumference of the airfoil (body). The profile drag coefficient includes viscous effects. These effects are *not* included in the form (pressure) drag coefficient.

The profile drag coefficient of a two dimensional airfoil is obtained by applying the linear momentum theorem to a control volume enclosing both the airflow over the airfoil and its wake. The net momentum deficit in the streamwise direction in the wake compared to the momentum in the free stream ahead of the airfoil gives the profile drag of the airfoil. The skin friction drag may be inferred from the calculated results for form and profile drags, i.e.

$$\text{skin friction drag} = \text{profile drag} - \text{form drag}$$

IV. Theory

Application of Linear Momentum Theorem: Wake Survey

Newton's second law applied to a homogeneous fluid enclosed in an arbitrary control volume as shown in Fig. 2–1 provides the basis for the linear momentum theorem.

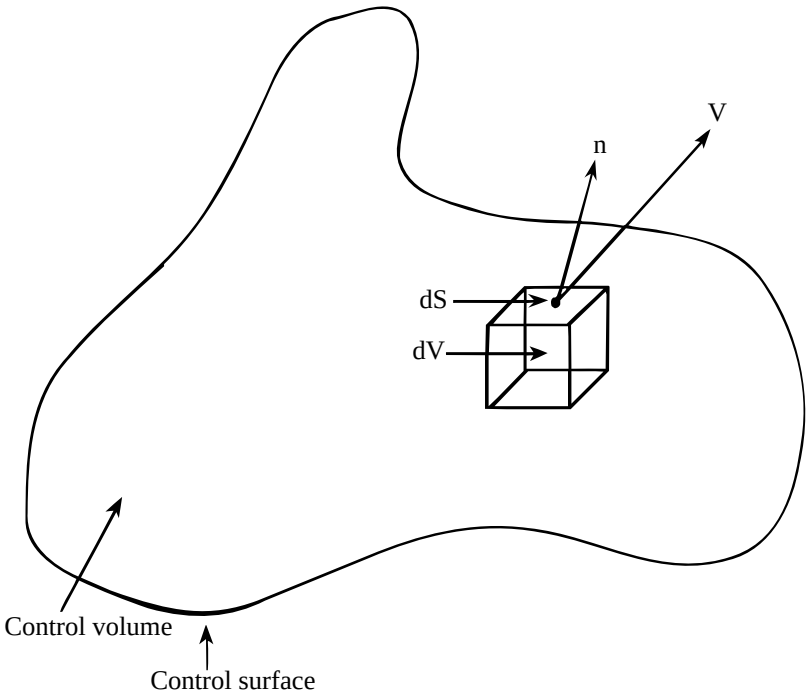

Figure 2–1. Sketch of a fluid element in a control volume.

According to the law of conservation of momentum, the net rate of change of the momentum of the fluid crossing a control volume bounded by a control surface is equal to the sum of all external forces acting on the control volume. This is expressed as

$$\sum \mathbf{F}_{\text{ext}} = \frac{\partial}{\partial \text{t}} \iiint_{\text{CV}} \rho \bar{V} dv + \iint_{\text{CS}} \rho \bar{V} (\bar{V} \cdot \bar{n}) dS \tag{1}$$

where ρ is the fluid density, $\mathbf{V}$ is the fluid velocity entering or leaving the control surface (CS) depending on whether $\mathbf{V} \cdot \mathbf{n}$ is negative or positive and $\mathbf{n}$ is a local unit outward normal vector to an element of area dS of the control surface. $\sum \mathbf{F}_{\text{ext}}$ is the resultant of all surface forces (pressure and shear) and all body forces (gravity). The linear momentum theorem is a statement of Eq. (1) which is an instantaneous vector relation balancing the sum of the time rate of change of momentum enclosed within the control volume and the net flux of momentum through the control surface enclosing the control volume with the resultant of the external forces applied to the control volume. Eq. (1) represents the linear momentum equation for a general three dimensional unsteady compressible flow.

As an application of the linear momentum theorem, the momentum equation, Eq. (1), is applied to a control volume enclosing a fluid flowing over a ceiling-to-floor mounted constant section airfoil and its wake. Looking down at the test section from above, the control volume (dashed lines) is bounded on the inside by the surface of the airfoil, on the outside by streamlines equally distant from the tunnel walls and outside the tunnel wall boundary layer and upstream and downstream lines normal to the streamlines labeled 1 and 2 in Fig. 2–2.

Because of viscous effects, a wake of retarded flow exists behind the airfoil in

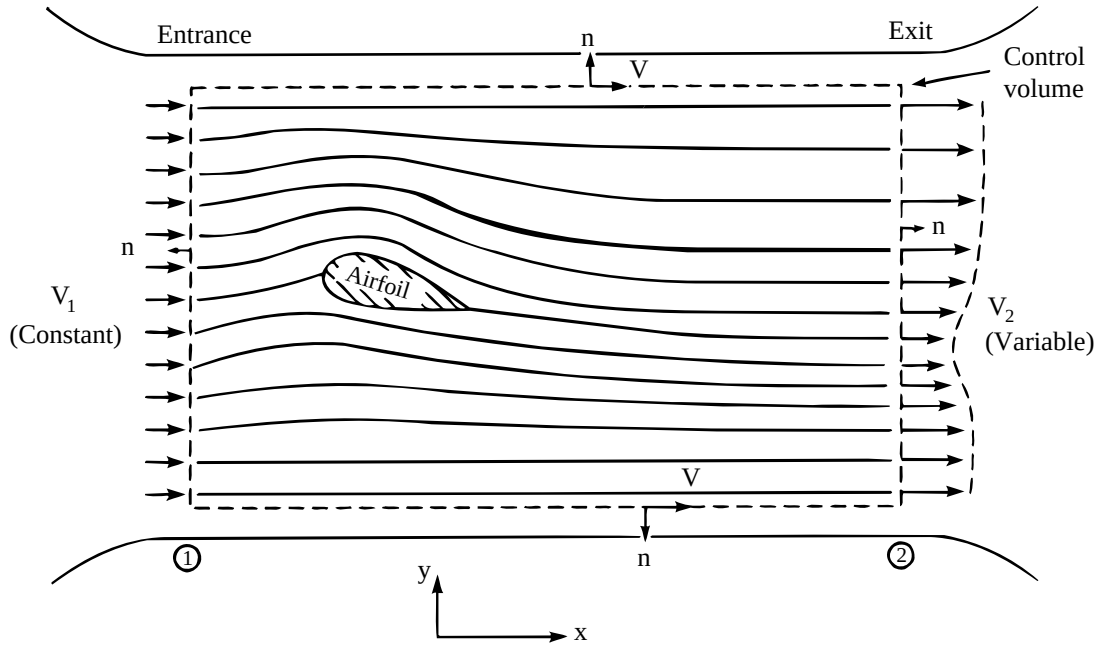

Figure 2–2. Drag of an airfoil from wake measurements.

Fig. 2–2. In the wake region, the velocity is less than the upstream value and varies across the test section, as illustrated by the profile at the right. Writing the x component of the momentum equation, Eq. (1), we have

$$\sum \mathrm{F}_{\mathrm{ext}_x} = \frac{\partial}{\partial \mathrm{t}} \iiint_{\mathrm{CV}} \rho V_x dv + \iint_{\mathrm{CS}} \rho V_x V_n dS \tag{2}$$

where the subscript x indicates the streamwise component of a vector and $V_n = \mathbf{V} \cdot \mathbf{n}$ is the normal component of the velocity vector at the control surface.

Now let us consider all the external forces on the control volume in the x direction, i.e.

$$\sum \mathrm{F}_{\mathrm{ext}_x} = p_1 A_1 - p_2 A_2 + F_x \tag{3}$$

where $p_1 A_1$ and $p_2 A_2$ are the pressure forces at the entrance and exit areas A_1 and A_2. The entrance and exit areas are assumed equal. F_x is the x component of the resultant force (due to viscous and pressure forces on the airfoil) exerted by the airfoil on the fluid in the control volume. F_x is equal and opposite to the force exerted by the control volume on the airfoil. This equal and opposite force is the aerodynamic drag on the airfoil, D. Note that the gravity force has no component in the x direction. Because the control surface is chosen outside the wall boundary layers, Eq. (3) excludes the tunnel wall shear forces,

The choice of stations 1 and 2 is arbitrary. However, a judicious choice of their locations eliminates the contribution of the pressure forces in Eq. (3). Station 1 can be placed relatively far upstream in the test section where the pressure is uniform and equal to the freestream static pressure ($p_1 = p_\infty$). The location of station 2 should be at a distance downstream from the airfoil trailing edge such that the pressure p_2 is also equal to $p_1 = p_\infty$. Measurements behind airfoils at low angles of attack (see Kuethe and Chow, 1986, p. 67) show that if station 2 is placed at least 12% of the airfoil chord behind the trailing edge, the pressure variation is small enough that $p_2 = p_1 = p_\infty$. Eq. (3) then reduces to

$$\sum \mathrm{F}_{\mathrm{ext}_x} = F_x = -D \tag{4}$$

which gives the drag force on the airfoil to within a few percent of its correct value.

Because the flow is steady, the first term on the right-hand side of Eq. (2) is zero. Combining Eqs. (3) and (4), the momentum equation then reads

$$-D = \iint_{\mathrm{CS}} \rho V_x V_n dS \tag{5}$$

Figure 1 shows that $V_n = \mathbf{V} \cdot \mathbf{n}$ is zero on the upper and lower control surfaces. Equation (5) then reduces to

$$-D = \iint_{\mathrm{CS}_1} \rho_1 V_1 (-V_1) dS_1 + \iint_{\mathrm{CS}_2} \rho_2 V_2 (+V_2) dS_2 \tag{6}$$

and assuming that the flow is incompressible ($\rho_1 = \rho_2 = \rho = \text{const}$) we have

$$-D = \rho \iint_{CS_2} V_2^2 dS_2 - \rho \iint_{CS_1} V_1^2 dS_1 \tag{7}$$

Using the continuity equation for one-dimensional steady incompressible flow, i.e.

$$V_1 dS_1 = V_2 dS_2 \tag{8}$$

and making a change of variable in the second integral of Eq. (7), i.e.

$$dS_1 = \frac{\mathrm{V}_2}{\mathrm{V}_1}\, dS_2 \tag{9}$$

the two integrals in Eq. (7) combine into one integral over CS_2 to yield

$$-D = \rho \iint_{CS_2} (V_2^2 - V_1 V_2) dS_2 \tag{10}$$

Introducing the nondimensional drag coefficient, with $V_1 = V_\infty$, yields

$$C_d \equiv \frac{\mathrm{D}}{\mathrm{q}_\infty \mathrm{S}} = \frac{\mathrm{D}}{{}^1\!/_2 \rho \mathrm{V}_\infty^2 \mathrm{bc}} = \frac{\rho \iint_{CS_2} (\mathrm{V}_\infty \mathrm{V}_2 - \mathrm{V}_2^2) \mathrm{dS}_2}{{}^1\!/_2 \rho \mathrm{V}_\infty^2 \mathrm{bc}} \tag{11}$$

where b is the wing span, c is the wing chord length, q_∞ is the upstream dynamic pressure, and $S = bc$ is the wing area of the constant cross section. The surface integral in Eq. (11) is transformed to a line integral by realizing that $dS_2 = b dy$, which yields

$$C_d = 2 \int_0^{y_{\max}/c} \left[\frac{\mathrm{V}_2}{\mathrm{V}_\infty} - \left(\frac{\mathrm{V}_2}{\mathrm{V}_\infty} \right)^2 \right] d\left(\frac{\mathrm{y}}{c} \right) \tag{12}$$

where $y = 0$ is the location of the lower wall, and $y_{\max}$ is that of the upper wall. In terms of the normalized dynamic pressure at station 2, we equivalently have

$$C_d = 2 \int_0^{\text{wall}} \left[\left(\frac{\mathrm{q}_2}{\mathrm{q}_\infty} \right)^{1/2} - \frac{\mathrm{q}_2}{\mathrm{q}_\infty} \right] d\left(\frac{\mathrm{y}}{\mathrm{c}} \right) \equiv C_{d_0} \tag{13}$$

This is the profile (pressure and viscous) drag coefficient of a two dimensional airfoil. The quantities required for evaluation of Eq. (13) are usually obtained from a "rake" composed of small pitot tubes spaced one to two tube diameters apart, with the pitot tube orifice about one chord length ahead of the rake body. The pitot tubes are individually connected to a multiple manometer. The dynamic pressure distribution in a typical wake is shown in Fig. 2–3.

Because only the ratio q_2/q_∞ is required, the readings are independent of the specific gravity of the manometer fluid. The constant readings of the outside tubes indicate that they are out of the wake and hence may be used to determine q_∞. In

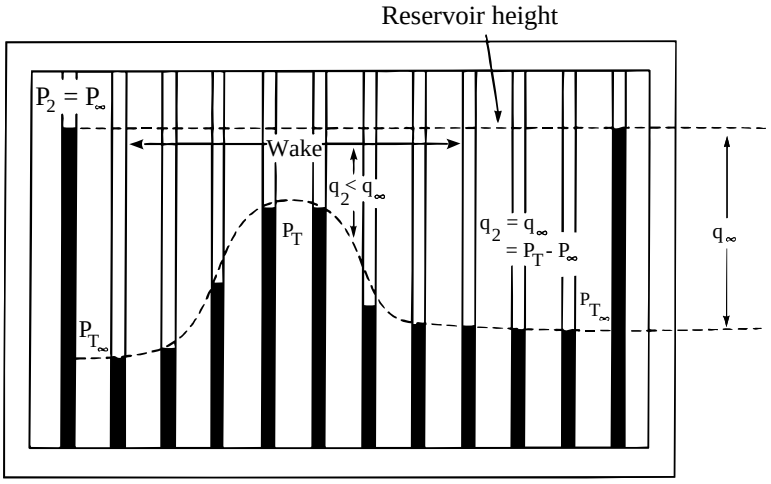

Figure 2–3. The wake as it appears on a multiple manometer.

practice, for low and moderate angles of attack, the rake is placed at 70% chord length behind the trailing edge of the wing, assuming that the static pressure in the wake is not far off from the freestream value p_∞. A typical plot of $\sqrt{q_2/q_\infty} - q_2/q_\infty$ versus y/c is shown in Fig. 2–4.

According to Eq. (13), the profile drag coefficient is equal to twice the area under the curve in Fig. 2–4. Any numerical or graphical integration scheme should give the value of the area under the curve. In particular, the trapezoidal rule can be used to numerically or graphically evaluate the integral in Eq. (13).

The wake survey method cannot be used to measure the drag of stalled airfoils (high angle of attack) or of airfoils with flaps extended. Under these conditions, a large part of the drag is caused by rotational losses and does not appear as a change in linear momentum.

Surface Pressure Distribution on a Two Dimensional Wing

If the pressure distribution is known at all points along the surface of an airfoil,

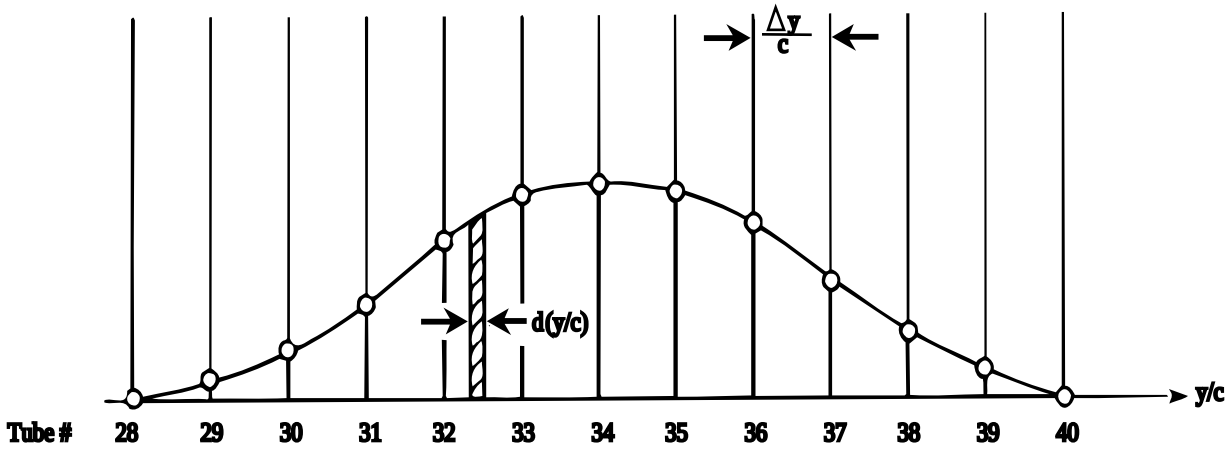

Figure 2–4. Integrand of drag integral of Eq. (13).

whether determined from actual measurements or from potential flow theory, an integration can be performed to calculate the overall pressure force on the body. It is convenient to determine components of this force in the chordwise and normal direction. From Fig. 2–5 we have

$$L = N\cos\alpha - C\sin\alpha \tag{14}$$

$$D = N\sin\alpha + C\cos\alpha \tag{15}$$

where N, C, L, and D are the normal, chordwise, lift and drag forces, respectively and α is the two dimensional geometric angle of attack. Nondimensionalizing these forces by the freestream dynamic pressure, q_∞, and the wing planform area, S, Eqs. (14) and (15) yield in coefficient form

$$C_l = C_n\cos\alpha - C_c\sin\alpha \tag{16}$$

$$C_d = C_n\sin\alpha + C_c\cos\alpha \tag{17}$$

At small angles of attack the chordwise force coefficient, C_c, is very small compared to the normal force coefficient, C_n; and because $\sin\alpha$ is much smaller than $\cos\alpha$, the cumulative order of magnitude of the product $C_c\sin\alpha$ is much smaller than $C_n\cos\alpha$. Hence, we neglect the $C_c\sin\alpha$ term and Eq. (16) reduces to

$$C_l = C_n cos\alpha \tag{18}$$

However, both terms on the right hand side of Eq. (17) are of the same order of magnitude and must be retained. Note that the drag coefficient, C_d, in Eq. (17) is due only to surface pressure distribution and does not include the skin friction drag.

In order to determine the normal and chordwise force coefficients, we consider the effect of pressure on the upper and lower surfaces of elemental areas at the same chordwise location on the airfoil, as shown in Fig. 2–6. In Fig. 2–6 the x- and y-axes are the chordwise and normal directions of the pressure forces and b is the

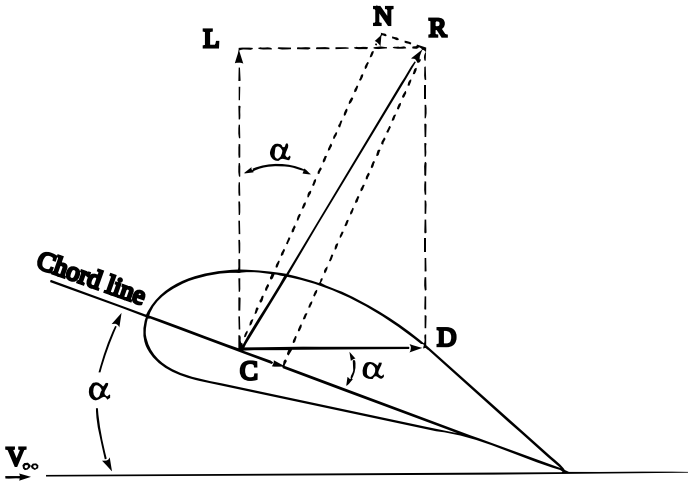

Figure 2–5. Forces on an airfoil.

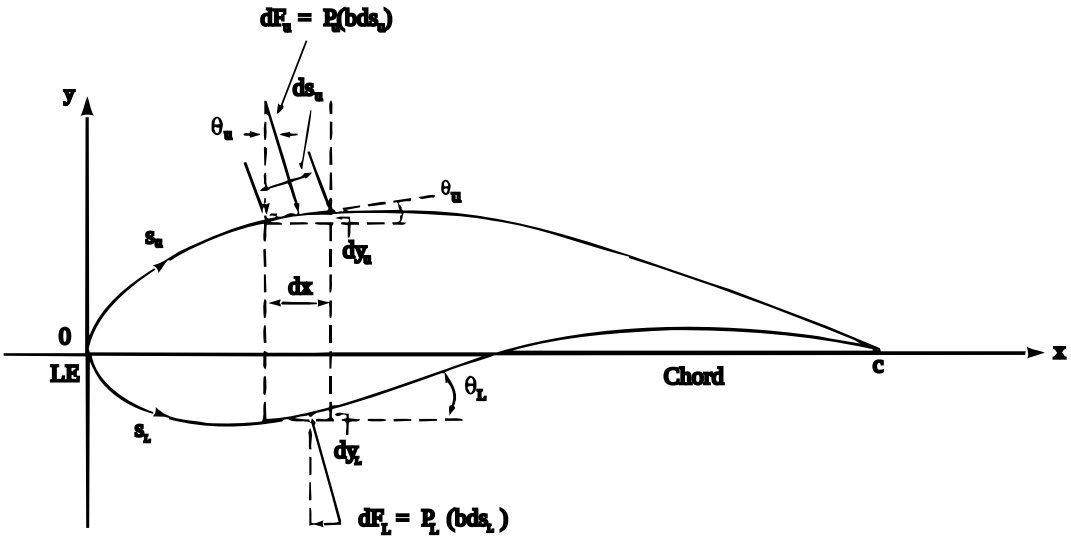

Figure 2–6. Elemental forces on the upper and lower surface of an airfoil.

wing span. The upper and lower surfaces are referred to by the subscripts u and L, respectively. dF_u and dF_L are the elemental upper and lower pressure forces acting on elemental areas bds_u and bds_L, respectively, s_u and s_L are the upper and lower curvilinear coordinates of a point on the airfoil surface at the same x location. Both are measured from the leading edge of the airfoil. The chordwise elemental pressure force, dF_x, is the sum of both upper and lower chordwise elemental pressure forces at the same x location, i.e.

$$dF_x = p_u(bds_u)\sin\theta_u + p_L(bds_L)\sin\theta_L \tag{19}$$

But
$$dy_u = ds_u \sin\theta_u \quad dy_L = ds_L \sin\theta_L \tag{20a,b}$$

which are the x projections of ds_u and ds_L along the y-axis. θ_u and θ_L are the angles of the slopes of ds_u and ds_L, which in general are not equal. However, for symmetric airfoils, $ds_u = ds_L$ and $\theta_u = \theta_L$ so that $dy_u = dy_L$. For nonsymmetric airfoils with small camber, $dy_u \approx dy_L$. Under these conditions, Eqs. (19) and (20) yield

$$dF_x = b(p_L + p_u)dy \tag{21}$$

where $dy = dy_u = dy_L$. Similarly, the normal elemental pressure force dF_y can be expressed as

$$dF_y = -p_u(bds_u)\cos\theta_u + p_L(bds_L)\cos\theta_L \tag{22}$$

or
$$dF_y = b(p_L - p_u)dx \tag{23}$$

where
$$dx = ds_u\cos\theta_u = ds_L\cos\theta_L \tag{24}$$

The relations in Eq. (24) are exact regardless of symmetry. Introducing the nondimensional pressure coefficient

$$C_p \equiv \frac{\mathrm{p} - \mathrm{p}_\infty}{\mathrm{q}_\infty} \tag{25}$$

and integrating the forward (FWD) and aft (AFT) chordwise pressure forces with respect to the position of the maximum thickness of the airfoil, we obtain

$$\begin{aligned}
F_x &= b\int_0^{y_{\max}} (p_L + p_u)_{\text{FWD}}\, dy + b\int_{y_{\max}}^{0} (p_L + p_u)_{\text{AFT}}\, dy \\
&= bq_\infty \int_0^{y_{\max}} \left[\frac{\mathrm{p_L - p_\infty}}{\mathrm{q_\infty}} + \frac{\mathrm{p_u - p_\infty}}{\mathrm{q_\infty}} + \frac{\mathrm{2p_\infty}}{\mathrm{q_\infty}} \right]_{\text{FWD}} dy \\
&\quad - bq_\infty \int_0^{y_{\max}} \left[\frac{\mathrm{p_L - p_\infty}}{\mathrm{q_\infty}} + \frac{\mathrm{p_u p_\infty}}{\mathrm{q_\infty}} + \frac{\mathrm{2p_\infty}}{\mathrm{q_\infty}} \right]_{\text{AFT}} dy \\
&= bq_\infty \int_0^{y_{\max}} \left(C_{p_L} + C_{p_u} + \frac{\mathrm{2p_\infty}}{\mathrm{q_\infty}} \right)_{\text{FWD}} dy - bq_\infty \int_0^{y_{\max}} \left(C_{p_L} + C_{p_u} + \frac{\mathrm{2p_\infty}}{\mathrm{q_\infty}} \right)_{\text{AFT}} dy \\
&= bq_\infty \int_0^{y_{\max}} \left[\left(C_{p_L} + C_{p_u} \right)_{\text{FWD}} - \left(C_{p_L} + C_{p_u} \right)_{\text{AFT}} \right] dy
\end{aligned} \tag{26}$$

where the third terms in the integrands cancel because they are equal and constant. $y_{\max}$ is the maximum ordinate of the upper surface of the airfoil. It is equal to the half of the maximum thickness of a symmetric airfoil.

The chordwise force coefficient for a rectangular wing is

$$C_c = \frac{F_x}{q_\infty S} = \frac{F_x}{q_\infty bc} = \int_0^{t_{\max}} \left[\left(C_{p_L} + C_{p_u} \right)_{\text{FWD}} - \left(C_{p_L} + C_{p_u} \right)_{\text{AFT}} \right] d\left(\frac{y}{c}\right) \tag{27}$$

where $t_{\max} = \mathrm{y_{max}/c}$ is half the maximum thickness ratio of the airfoil.

Similarly, integrating the normal pressure forces we obtain

$$\begin{aligned}
F_y =& b\int_0^c (p_L - p_u)dx = q_\infty b \int_0^c \left(\frac{p_L - p_\infty}{q_\infty} - \frac{p_u - p_\infty}{q_\infty} \right) dx \\
=& q_\infty b \int_0^c (C_{p_L} - C_{p_u})dx
\end{aligned} \tag{28}$$

The normal force coefficient for the special case of a rectangular wing is then

$$C_n = \frac{F_y}{q_\infty S} = \frac{F_y}{q_\infty bc} = \int_0^1 (C_{p_L} - C_{p_u}) d\left(\frac{x}{c}\right) \tag{29}$$

The integral of Eq. (29) represents the area between the pressure coefficient curves as shown in Fig. 2–7. Positive contributions occur when lower surface pressures are more positive than upper surface pressures.

Thus, to determine the normal force coefficient, local pressure coefficients are plotted perpendicularly to the chord line at the local y_c location (see also Fig. 2–8b).

To determine the chordwise force coefficient of Eq. (27), C_p values are plotted parallel to the chord line at the local $\mathrm{y/c}$ location (Fig. 2–8c). The chordwise coefficient is positive when forward pressures are greater than aft pressures. Note that the chordwise force is due solely to surface pressure distribution and does not include skin friction forces. Therefore, we use the wake survey analysis to experimentally determine the sectional profile drag coefficient which includes the skin friction drag.

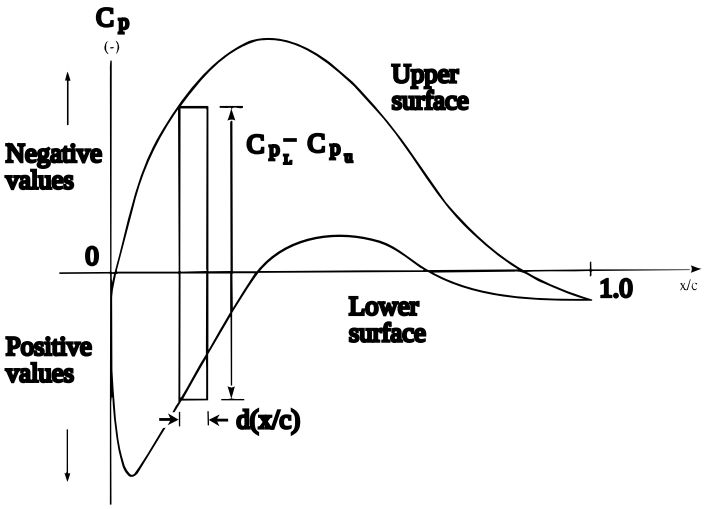

Figure 2–7. Typical C_p distribution on the upper and lower surface.

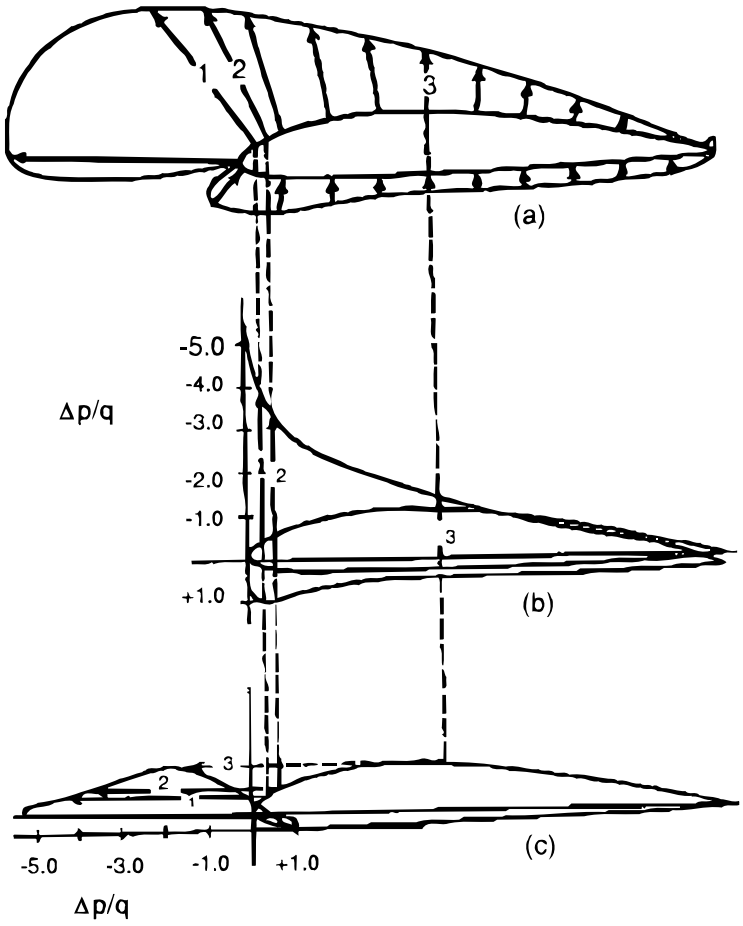

Figure 2–8. The actual pressure distribution and its presentation.

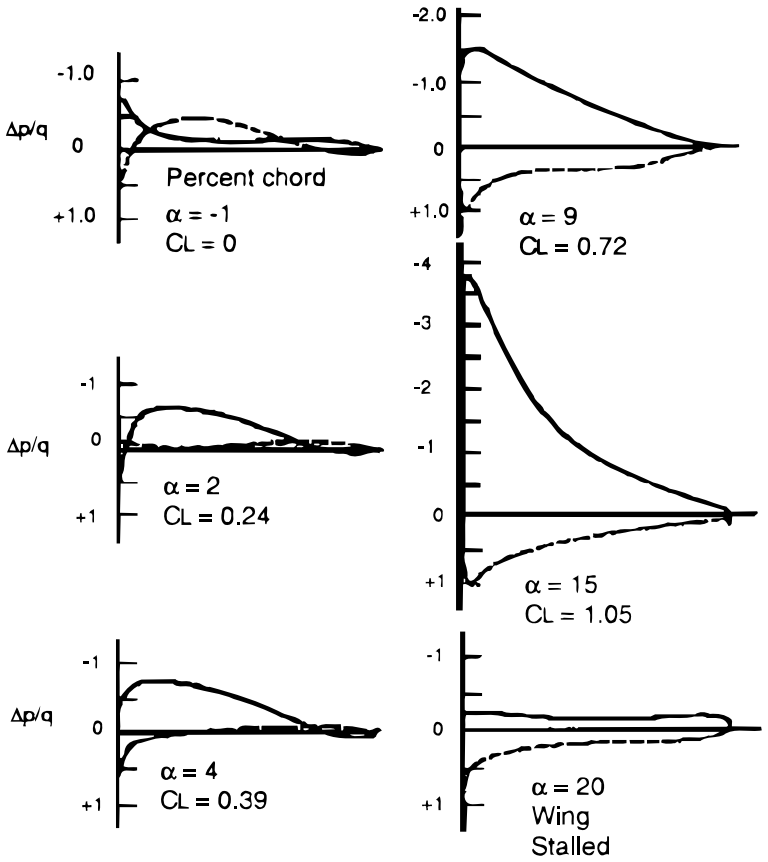

Figure 2–9. Growth of the static pressure distribution with angle of attack.

The growth of the pressure distribution with increasing angle of attack for a typical airfoil is shown in Fig. 2–9.

In addition to lift and drag coefficients, the pitching moment about some arbitrary point on the airfoil can be determined from the pressure distribution. Taking moments about the leading edge and converting to coefficient form yields

$$C_m = \frac{m(0)}{q_\infty xc} = \int_0^1 (C_{p_u} - C_{p_L})\left(\frac{x}{c}\right) d\left(\frac{x}{c}\right) + \int_0^1 (C_{p_u} + C_{p_L})\left(\frac{y}{c}\right) d\left(\frac{y}{c}\right) \tag{30}$$

which is taken to be positive when the nose, i.e., the leading edge, pitches upward. The moment about any other point $^{x}/_{c} = h$ is obtained from

$$C_m(h) = C_m(c) + hC_n \tag{31}$$

where the small angle assumption has been made in order to neglect the C_c contribution. The integrals in Eq. (30) may be evaluated from the area under curves of $(C_{p_u} - C_{p_L})(^{x}/_{c})d(^{x}/_{c})$ and $(C_{p_u} + C_{p_L})(^{y}/_{c})d(^{y}/_{c})$

V. Physical Set-up

A symmetrical NACA 63-012 airfoil with a 12 inch chord is vertically mounted in the test section of the wind tunnel. Forty (40) pressure taps are symmetrically arranged

at the center of the span. The pressure taps are flush with the surface. Pressure measurements are recorded digitally with a scani-valve. The airfoil can be rotated about a vertical axis.

A wake rake containing pitot tubes is mounted one chord length behind the airfoil. Two static pressure tubes are mounted at the extremes of the rake and approximately one inch above and below the plane of the rake. Note that the wake rake aft of the wing does not affect the results upstream.

VI. Procedure

1. Make the usual measurements of barometric pressure and temperature.
2. Stabilize the wind tunnel at an inclined manometer reading of 8 inches alcohol.
3. Set the angle of attack at zero, $\alpha = 0$, then note the tare reading to see whether the upstream flow is indeed approaching the airfoil at zero degrees or at a slight angle. To determine the true zero angle of attack of the symmetrical airfoil at a given tunnel speed, adjust the angle of attack until the pressure distribution appears symmetrical, i.e., the top and bottom pressures are equal at the same chordwise location.
4. Vary the angle of attack from $-6°$ to stall in two degree increments. Record the following data for each run:
   a. Freestream static pressure.
   b. Surface static pressure distribution on the airfoil.
   c. The total pressure distribution across the wake.
   d. The temperature at the end of each run.

VII. Results Required

1. A scaled drawing of the NACA wing section showing the location of all pressure taps.
2. Evaluate and plot the experimental distributions of C_p vs $^{x}/_{c}$ at each angle of attack.
3. Compare the plots for the experimental and NACA 63-012 C_p distributions vs $^{x}/_{c}$ at zero angle of attack.
4. Calculate and plot the sectional lift coefficient, C_l and the form drag coefficient C_d vs angle of attack. Compare the experimental results to those for an NACA 63-012 airfoil as give in *Theory of Wing Sections*. Explain any differences.
5. For each angle of attack plot $\sqrt{q_2/q_\infty} - q_2/q_\infty$ vs $^{y}/_{c}$ and evaluate the profile drag coefficient C_{d_0}.
6. Plot C_{d_0} and C_{d_f}, the skin friction drag coefficient vs angle of attack.
7. Compare the experimental and NACA results for C_{d_0} vs α. Note that because the NACA data in *Theory of Wing Sections* is given for different Reynolds numbers and the experimental data must be compared at the same Reynolds

number, it may be necessary to apply the following empirical formula applicable only to C_{d_0}

$$C_{d_{0_1}} = C_{d_{0_2}} \left(\frac{\mathrm{Re}_2}{\mathrm{Re}_1} \right)^{0.11} \tag{31}$$

where $C_{d_{0_2}}$ is the experimental profile drag coefficient at Re_2, and $C_{d_{0_1}}$ is the scaled value of $C_{d_{0_2}}$ at the Reynolds number Re_1 of the NACA data.

Pressure Tap Locations for the NACA 63-012 Wing Section

Top Surface			Bottom Surface		
Tap	% x/c	% y/c	Tap	% x/c	% y/c
1	0.00	0.0			
2	0.40	1.1	3	0.5	1.2
4	1.08	1.5	5	1.0	1.5
6	1.80	2.0	7	2.0	2.0
8	2.80	2.4	9	3.0	2.4
10	3.70	2.7	11	4.0	2.8
12	4.90	3.1	13	5.0	3.1
14	10.00	4.2	15	10.0	4.1
16	14.80	4.8	17	1.5	4.6
18	20.00	5.4	19	20.0	5.4
20	25.90	5.5	21	25.0	5.8
22	29.90	5.9	23	30.0	5.9
24	34.90	6.0	25	35.0	6.1
26	39.90	5.9	27	40.0	6.0
28	49.60	5.4	29	50.0	5.4
30	59.60	4.4	31	60.0	4.5
32	69.50	3.2	33	70.0	3.3
34	79.50	1.9	35	80.0	1.9
36	89.50	0.7	37	90.0	0.8
38	94.40	0.3	39	95.0	0.4
			40	100	0.0

VIII. Homework Assignment

An airfoil with a 6 inch chord is mounted in the USNA recirculating wind tunnel. A wake rake is mounted one chord length behind the airfoil. The rake has both pitot and static pressure tubes for freestream reference and 8 pitot tubes that measure the wake momentum deficit via total pressures. The rake is attached to an alcohol (s.g. = 0.806) manometer board.

Manometer tubes #1 and #2 are attached to the static and total head ports, respectively, while tubes #3 through #10 are pitot tubes spanning the wake. Laboratory conditions are $P_{atm} = 30.03\,\mathrm{in\,Hg}$ and $T = 75°\mathrm{F}$. The tunnel temperatures

were 75° and 95° at the beginning and end of the test run, respectively. The readings on the manometer board are listed below:

Tube	h(in)
1	6.00
2	0.00
3	2.08
4	3.69
5	4.88
6	5.00
7	4.87
8	3.70
9	2.10
10	0.01

Assume the space between the tubes is uniform and equal to the a tenth of the chord length.

1. Tabulate and plot the function $\sqrt{q_2/q_\infty} - q_2/q_\infty$ vs y/c for the wake.
2. Calculate the profile drag coefficient of the airfoil using the trapezoidal rule.

EA303 WIND TUNNEL
EXPERIMENT II

TWO DIMENSIONAL
WING PRESSURE DISTRIBUTION AND WAKE SURVEY

Pressure Tap Setup

The pressure taps on the airfoil are lead to a multiple manometer and also through a scanning valve to a pressure transducer. The values from the pressure transducer are read by a digital data acquisition system (computer). The correspondence between the pressure ports and the individual tubes of the multimanometer as well as the numbering system for the digital data acquisition system are shown in Fig. 2–10

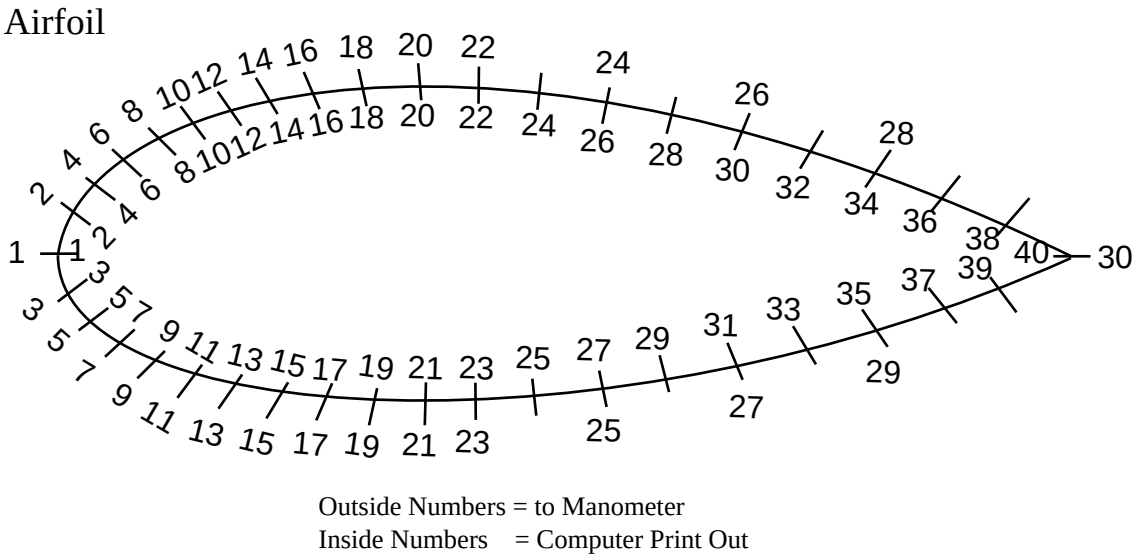

Figure 2–10. Airfoil pressure numbering system.

Similarly the pitot and static pressure tubes in the wake rake are connected to both a multimanometer and to the digital data acquisition system. The numbering system is shown in Fig. 2–11.

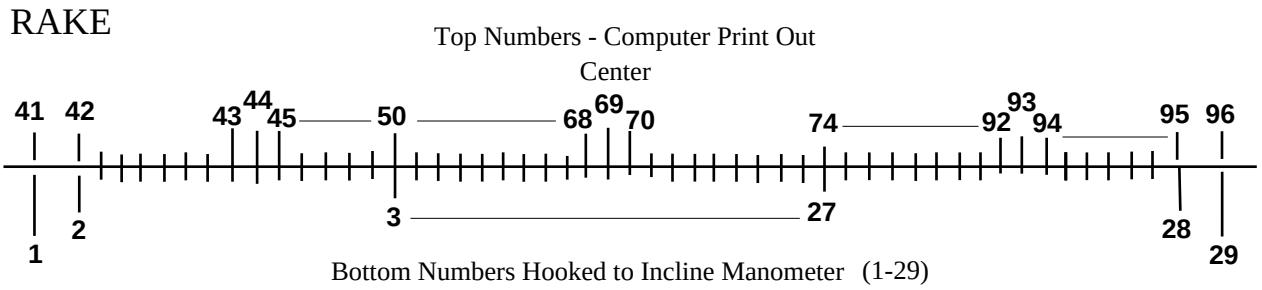

Figure 2–11. Wake rake pressure numbering system.